Tunneling time of long-wavelength phonons through semiconductor heterostructures

Diosdado Villegas*
Physics Department, Central University "Marta Abreu" of Las Villas, Santa Clara, Cuba

Fernando de León-Pérez†
Institut für Theoretische Physik III, Universität Stuttgart, Pfaffenwaldring 57, D-70550 Stuttgart, Germany

Rolando Pérez-Alvarez‡
Physics Faculty, Havana University, 10400 Havana, Cuba
(Received 7 June 2004; published 19 January 2005)

A characteristic time for the tunneling of long-wavelength phonons through nonpolar semiconductor heterostructures is derived from the energy density continuity equation of the system. It is a mathematical analog of the well known dwell time for electrons. We study the tunneling of optical and acoustic phonons at normal incidence on multiple layers systems. A relation between the dwell time and the phase times for phonons which is similar to that obtained for electrons is deduced. At the same time the phase times for acoustic phonons are generalized to include the optical phonons. Our findings could be easily extrapolated to both the particle and electromagnetic wave tunneling. This study could also be useful for the design of phonon optics devices.

DOI: 10.1103/PhysRevB.71.035322 PACS number(s): 68.65.Cd, 63.20.Dj, 63.22.+m

I. INTRODUCTION

The tunneling time of electrons through a potential barrier have been a long standing question for physicists and still remains controversial. There is not a unique definition for the tunneling time up to now.[1–4] A direct experimental study is not straightforward for the barrier traversal time of electrons is orders of magnitude shorter—of the order of 10^{-14}–10^{-15} s—than the highest time resolution achievable in electronics.[5] In fact, very few experiments provide some indirect information about the temporal dynamics of particle tunneling. Instead, some general trends can be extrapolated from optical experiments. Martin and Landauer have shown that the one-dimensional particle tunneling is in direct analogy with evanescent electromagnetic (EM) waves found in a low-dielectric-constant region separating two regions of higher dielectric constant.[6] Accurate measurements of single-photon and optical-pulse delay times in the photonic band gap of multilayer media,[7–11] in wave guides operating below cutoff,[12,13] and for frustrated total internal reflection experiments,[14] have stimulated the interest in studying the tunneling time—mainly the superluminal barrier tunneling—up to the present time.[15]

In a series of recent interesting papers, Winful has argued that the time delays for EM waves are not propagation delays and should not be related to a velocity.[16–19] He has shown that the phase time is proportional to the average time in which the energy is stored in the cavity and it is a measure of the cavity lifetime for the EM wave. He used this proportionality between the phase time and the stored energy to explain the paradox of the Hartman effect[20] for EM waves. For the photonic band gap structures studied in Refs. 16 and 17 the dwell time, t_D, was shown to be equal the phase time, τ_t, as a consequence of the nondispersive plane wave propagation characteristic of these EM waves. In a simulation based on EM field equations for the photonic band gap structure Winful has shown that the peak of the tunneling wave packet does not propagate from input to output.[17,18] Output and input wave packet peaks are therefore not related by causal propagation and hence the phase time is not a propagation delay. These simulations could be easily extrapolated to the electron tunneling. Similar studies with the Dirac equation also show an absence of a wave packet peak in the barrier during tunneling.[21] With these simulations in mind, Winful has exploited the analogy between EM waves in band gap structures and the electrons to show that the Hartman effect can be explained by the saturation of the integrated probability density (or number of particles) under the barrier.[22] After some algebra with the time-independent Schrödinger equation, he derived a relation between the dwell time and the phase times, previously obtained by Hauge *et al.* using a wave packet analysis.[23] This relation reads

$$t_D = \tau_t \mathcal{T} + \tau_r \mathcal{R} + t_i, \tag{1}$$

where τ_r is the reflexion phase time, $\mathcal{T}$ and $\mathcal{R}$ are the transmission and reflexion coefficients, respectively, and t_i is a self-interference term that comes from the overlap of the incident and the reflected waves in front of the barrier. The dwell time for a particle in the barrier region $0<x<L$ is defined in accordance with Refs. 24 and 25 as

$$t_D = \frac{\int_0^L |\psi(x)|^2 dx}{j_{in}}, \tag{2}$$

where $\psi(x)$ is the stationary state wave function and j_{in} is the flux of the incident particle. Falck and Hauge have shown that for symmetric scattering potentials $\tau_t = \tau_r$.[26] Thus, the expression for t_D simplifies to

$$t_D = \tau_t + t_i. \tag{3}$$

In this paper only symmetric potentials are considered for the sake of convenience.

A time which does not saturate with barrier length is obtained after dividing the integrated particle density by the flux within the barrier (that arises from the interference between evanescent and antievanescent modes), i.e., dividing the previous expression for t_D by the transmission coefficient $\mathcal{T}$. It was intuitively proposed by Moura and Albuquerque.[27] Winful named it as perfectly "luminal" net-flux delay τ_D^N,[22] in the sense that it does not suffer from the paradoxical Hartman effect. Thus

$$t_D^N = \frac{t_D}{\mathcal{T}}. \tag{4}$$

With this redefinition of the dwell time the aforementioned derivation of the relation (1) is still valid, when it is written as

$$t_D^N \mathcal{T} = \tau_t \mathcal{T} + \tau_r \mathcal{R} + t_i. \tag{5}$$

As Winful stated, this analysis is also valid for photons, with the condition $t_i = 0$. The above mentioned experiments with EM waves are designed to measure the group delay between incident and transmitted wave packets, i.e., the phase delay (and not the redefined dwell time). The experimental data is in agreement with theoretical calculations.[28,29] The net-flux delay can be computed from these experimental results.[22]

In this paper we show that for phonons a well-behaved dwell time like t_D^N in (4), i.e., which does not saturate with barrier length, can be derived directly from the energy density continuity equation, without any additional assumption. Consequently the label "net" is not used in the following. We also obtain the relation between dwell time and phase time for an arbitrary layered structure, casts in the form (5). Then a saturation of the vibrational energy stored in the barrier can be invoked to disregard paradoxically interpretations of phonon group velocities larger than the sound velocity in the solid. In fact, some nice experiments are presented in Ref. 30 showing the breaking of the sound barrier in solids.

We study long-wavelength phonons propagating along high symmetry directions in nonpolar semiconductors. Under these conditions the atomic oscillations are described by one-dimensional differential equations.[31] The results here obtained could be easily extrapolated to the tunneling of both EM and electrons. In fact the acoustic phonons are not dispersive (like EM waves in photonic band gap structures) while the optical phonons show a dispersive character (like electrons). For the sake of generality we write expressions valid for both optical and acoustic phonons. We find some analytical properties valid for an arbitrary number of barriers that, to the best of our knowledge, have not been considered before neither for electrons nor for EM waves. We also show that a more comprehensive picture of the tunneling time can be achieved by studying multibarrier systems with more than two barriers for the whole energy range. This picture is not clearly revealed in theoretical studies for electrons and EM waves—these studies considering together both the dwell and phase time—that are generally limited to two barriers or to some windows of the whole spectrum.

The phonon tunneling has been largely studied (see, for example, Refs. 32–35 and references therein). Also acoustic phonons have been proposed as an alternative to study the tunneling time. A few years ago Mizuno and Tamura[32] suggested—by considering that phonons travel at sound velocity, which is slower than the electron velocity, and taking also into account that its mean free path is macroscopic in pure samples and ranging in THz characteristic frequencies—that the measurement of the time delay or the advance of phonons in heterostructures is easier than in the case of electrons (see the discussion about it in Ref. 32). On the other hand, semiconductor heterostructures are useful for the design of various phonon optic devices such as phonon mirrors, phonon reflectors, phonon resonators, and so on.[36] Systems for phonons based on multiple superlattice (SL) structures have been proposed (see Ref. 32 and references therein). Tamura and Mizuno also studied the time evolution of acoustic phonon packets normally incident on the layer interfaces of superlattices.[34] A theoretical study of the group velocity of acoustic phonons in a finite superlattice is presented in Ref. 35. But neither of the previous papers have considered the dwell time, derived here, or its relation with the phase time. In addition, previous results of Mizuno and Tamura[32] for the phase times of acoustic phonons are generalized here in order to include optical phonons.

We consider in the following the phonons incident on a multiple-barrier structure consisting of an alternate stacking of the layers A and B. The system studied is expressed as $X(AB)^N Y$, where X and Y denote the substrate and detector layer, respectively. Their vibrational properties are assumed to be the same as that of layer B, and N is the number of the pair AB layers in the structure. We suppose the phonon propagation normal to the layer interfaces and adopt the continuum model valid for long wavelength oscillations. Under this assumption the acoustic and optical bulk dispersion relations are linear and parabolic, respectively.

The acoustic phonon dispersion relation in a periodic superlattice is obtained by folding the dispersion curves for the bulk materials back into the mini-Brillouin-zone (MBZ) determined by the periodicity of the superlattice. In the folded dispersion relation frequency gaps are generally formed at the center and at the boundary of the MBZ. We can control the size of the MBZ by changing the length of the unit period of the SL. On the other hand, for a finite superlattice with a small number of periods some resonances appear. Each state is duplicated N times when the number of periods increases N times (as a result of the hybridization of the modes in the different periods). For a given number of periods the phonon features are similar to the dispersion relation of the infinite periodic SL.[33] For the optical vibrations a similar behavior is found. Though in this case it is worth to recall that the bulk phonon branches for one material in the period does not overlap the branch of the other, instead a bulk phonon gap is present. Then, for optical phonons we differentiate the fre-

quency values for which the oscillations are allowed in both materials from these frequencies that are forbidden in one of the materials.

As mentioned above, nanostructures made of nonpolar semiconductors are ideal for our study. In particular, we consider the isotopic short period Ge multibarrier system, that have attracted the attention in the past years.[37] The phonon dispersions of two isotopic enriched Ge bulk materials overlap over a large frequency range (but confined optical modes are also present), and strain effects are not important. These structures are also grown in practice with almost ideal interfaces.

The paper is organized as follows. The main theoretical findings are presented in Sec. II, where the dwell time for phonon in heterostructures is derived from the energy density continuity equation. In Sec. III we computed the phase times valid for optical phonons, which includes previous results for acoustic phonons as a particular case. In Sec. IV we study the analytical relation between dwell time and phase times. This relation is deduced in the Appendix. An additional discussion of the analytical results and some numerical examples are given to Sec. V. At the end, the main conclusions are given in Sec. VI.

II. DWELL TIME

For high symmetry directions of the Diamond structure, like the [001] and [111] directions, the harmonic phonon equations of motion decouple into one longitudinal and two degenerated transverse oscillations, which are described by a linear chain model.[38] Phonons with wave vectors close to the center of the Brillouin zone[39] do not feel the discrete nature of the atomic structure, and for them the long-wavelength approximation is valid. In these conditions the discrete equations of motion transform to a continuum problem described by a second order differential system of equations.[31,40] The same equations are valid for both longitudinal and transverse vibrations and we will suppress these labels in the following. We write down formulas valid for optical phonons. These include the case of acoustic phonon with the appropriate selection of the parameters that will be shown below.[33] For the sake of convenience we formulate the problem with the help of its one-dimensional energy density

$$\mathcal{H} = \frac{1}{2}\rho \left| \frac{\partial u}{\partial t} \right|^2 + \frac{1}{2}\rho\omega_0^2|u|^2 + \frac{1}{4}\left[\sigma \frac{\partial u^*}{\partial x} + \sigma^* \frac{\partial u}{\partial x} \right], \quad (6)$$

and we write it for the stationary case. The first term in (6) represents the kinetic energy density, the second one represents the interaction energy density of the phonon field with itself, and the third one the strain energy density that accounts for the dispersive character of the oscillations. These terms depend on the atomic relative displacements u, the linear mass density ρ, the phonon frequency at the center of the Brillouin zone ω_0, the one-dimensional strain tensor $\partial u/\partial x$, and the stress tensor σ, which is equal to

$$\sigma = -\rho\beta^2 \partial u/\partial x, \quad (7)$$

where β is a parameter that accounts for the behavior of the bulk phonon dispersion relation.

From (6), the one-dimensional equation of motion[31] is easily obtained,

$$\frac{\partial^2 u}{\partial t^2} = -\omega_0^2 u - \beta^2 \frac{\partial^2 u}{\partial x^2}. \quad (8)$$

Note that the stationary solution of (8), i.e., a solution proportional to $e^{i\omega t}$ where ω is the mode frequency, leads to a Helmholtz equation which is equivalent to both the time-independent Schrödinger equation and the EM field equations.[6]

Using (8) it is possible to write the continuity equation for the energy density

$$\partial\mathcal{H}/\partial t + \partial j/\partial x = 0, \quad (9)$$

as a particular case of the developments presented in Ref. 33, where the energy density flux, j, is written as

$$j = -1/2(\sigma \partial u^*/\partial t + \sigma^* \partial u/\partial t). \quad (10)$$

For the stationary solution of the equation of motion it is straightforward to obtain that $\partial\mathcal{H}/\partial j = \mathcal{H}/j$, and that j does not depend on the coordinate x (we will return in Sec. II C to these statements). For this case, the continuity equation is integrated—taking into account that the infinitesimal increment dt_D is related to the infinitesimal increment of the total energy per unit of incoming energy density flux—to obtain

$$t_D = -\frac{H}{j}, \quad (11)$$

where H is the total energy in the interval $[x_1, x_2]$, obtained after the integration of (6), i.e.,

$$H = \int_{x_1}^{x_2} \mathcal{H} dx. \quad (12)$$

In the following we take (11) as the definition of the dwell time t_D. Note that j refers to the flux in the same interval where the energy H is computed. A minus sign in (11) is needed due to the energy density flux for optical phonons is negative, given the negative group velocity for the parabolic dispersion relation in the bulk, as shown below.

In order to obtain the equation for acoustic phonons we need to set to zero the constant ω_0, and make the replacement $\beta^2 \to -v^2$, where v is the sound velocity. Also ρ refers in this case to the total atomic mass density. For acoustic phonons the integration of (9) leads to $t_D = H/j$. For the sake of convenience, from now on we will write the expressions for optical phonons unless otherwise stated.

Note also that for an interval composed by the union of a set of nonintersecting intervals $[x_1, x_2] \cup [x_2, x_3] \cdots$, and when j remains constant (like in the stationary case we are considering), the dwell time is additive, i.e.,

$$t_D = t_D^{x_1,x_2} + t_D^{x_2,x_3} + \cdots , \tag{13}$$

a very convenient fact for the layered systems we are studying. Calculating the energy stored in each layer and the energy flux (which is unique to the structure) it is easy to obtain the dwell time.

While calculating the vibrational energy and the energy flux for bulk phonon modes it is worth noticing that they have different forms when considering propagating or forbidden states. In the next two sections we will give the form of these magnitudes and thereafter they will be used to calculate the dwell time.

A. Propagating states

We first consider some spatial region with constant material parameters and in the frequency range of allowed optical oscillations, i.e., with $w < w_0$. The solution for the equation of motion (8) reads in this case

$$u = [A_t e^{ikx} + A_r e^{-ikx}]e^{-i\omega t}, \tag{14}$$

where $k = \sqrt{(\omega_0^2 - \omega^2)/\beta^2}$ is the wave vector, and A_t, A_r are the coefficients of the solutions propagating to the right (transmitted) and to the left (reflected), respectively. For this solution the energy (12) in the interval $[x_1, x_2]$ is equal to

$$H = \rho\omega^2[|A_t|^2 + |A_r|^2]\Delta x + \rho\frac{\omega_0^2}{k}|A_t||A_r|[\sin(\alpha_t - \alpha_r + 2kx_2) - \sin(\alpha_t - \alpha_r + 2kx_1)], \tag{15}$$

where the coefficients are written in terms of their modules and phases, i.e., $A_t = |A_t|e^{i\alpha_t}$ and $A_r = |A_r|e^{i\alpha_r}$; and $\Delta x = x_2 - x_1$. On the other hand, for the energy density flux we obtain

$$j = -\rho\omega\beta^2 k[|A_t|^2 - |A_r|^2]. \tag{16}$$

B. Forbidden states

In a region of constant material parameters, for frequencies $w > w_0$, the oscillations are forbidden. The solution to the equation of motion (8) could be obtained from the solution to the propagating states (14) after the replacement $k = i\kappa$,

$$u = [A_t e^{-\kappa x} + A_r e^{\kappa x}]e^{-i\omega t}, \tag{17}$$

where now $\kappa = \sqrt{(\omega^2 - \omega_0^2)/\beta^2}$. It is important to notice that the substitution $k = i\kappa$ which leads us from (14) to (17) is useless to transform directly (15). It is necessary to calculate the vibrational energy starting from (6) using (12) to obtain

$$H = \rho\frac{\omega_0^2}{2\kappa}[|A_t|^2(-e^{-2\kappa x_2} + e^{-2\kappa x_1}) + |A_r|^2(e^{2\kappa x_2} - e^{2\kappa x_1})] + 2\rho\omega^2|A_t||A_r|\cos(\alpha_t - \alpha_r)\Delta x. \tag{18}$$

The energy density flux is now given as

$$j = 2\rho\omega\beta^2\kappa|A_t||A_r|\sin(\alpha_t - \alpha_r). \tag{19}$$

Nevertheless these differences, we find that the reported analytical expressions for the dwell time for forbidden states can be obtained from the corresponding expression for allowed states after the replacement $k = i\kappa$.

C. Heterostructures

For heterostructures with an arbitrary configuration of well-acting and barrier-acting materials the dwell time is the sum of the dwell time in each layer (11), (13). The expression for the allowed (15), (16) and the forbidden (18), (19) oscillations are used in this case. We suppose the heterostructure sandwiched between well-acting bulk materials, and that a phonon is incident from the heterostructure left side. Part of the energy is reflected at the heterostructure's left side and the other part is transmitted to the right side, according with the conservation of the energy density flux. In our stationary approach the energy density flux is independent on the coordinate and it is equal to the transmitted energy flux to the right of the heterostructure j_t. It is proportional to the transmission coefficient of the structure as can be seem from (16) or (19). The transfer matrix method is useful to compute the energy (15), (18). In our case, the reflection coefficient is zero at the right side of the heterostructure. We compute the coefficients in each layer starting from the right side, where all the coefficients are proportional to the transmission coefficient, or equivalently to the transmitted flux, j_t. Dividing H and j to compute t_D (11) the transmission coefficient is canceled in both the numerator and the denominator of t_D. That is quite significative because the transmission coefficient has peaks and valleys related to the bands and gaps of the phonon spectra[33] and these features are not reflected in the curve of t_D, which is smoother. Of course, some resonances are presented in this curve, as we will see later. This discussion also shows that for the stationary case the relation $\partial\mathcal{H}/\partial j = \mathcal{H}/j$ is valid.

III. PHASE TIME

In Ref. 33 the one-dimensional transmission and reflection coefficients are computed for a finite superlattice with an arbitrary number of periods. We calculate here further the phase times. The results are generalizations of the acoustic phonons studied in Ref. 32 in order to include optical phonons. The solution at the Y detector has a coefficient given by

$$A_t = \frac{2e^{-ik_2Nd}}{2C(N) - i\left[\left(\frac{\Upsilon_2}{\Upsilon_1}\chi + \frac{\Upsilon_1}{\Upsilon_2}\zeta\right)\right]S(N)}, \tag{20}$$

where the following expressions are taken from[33]

$$S(N) = \begin{cases} \dfrac{\sin N\vartheta}{\sin\vartheta} & \text{for } \left|\dfrac{\lambda+\mu}{2}\right| \leqslant 1, \\ \left(\dfrac{(\lambda+\mu)}{|\lambda+\mu|}\right)^{N+1}\dfrac{\sinh N\vartheta}{\sinh\vartheta} & \text{for } \left|\dfrac{\lambda+\mu}{2}\right| > 1, \end{cases} \tag{21}$$

$$C(N)=\begin{cases}\cos N\vartheta & \text{for } \left|\dfrac{\lambda+\mu}{2}\right|\leqslant 1,\\ \left(\dfrac{\lambda+\mu}{|\lambda+\mu|}\right)^{N}\cosh N\vartheta & \text{for } \left|\dfrac{\lambda+\mu}{2}\right|>1,\end{cases} \tag{22}$$

by definition

$$\cos\vartheta\equiv\frac{\lambda+\mu}{2}\quad \text{for}\left|\frac{\lambda+\mu}{2}\right|\leqslant 1, \tag{23}$$

$$\cosh\vartheta\equiv\left|\frac{\lambda+\mu}{2}\right|\quad \text{for}\left|\frac{\lambda+\mu}{2}\right|>1, \tag{24}$$

and

$$\lambda=\cos\alpha_1\cos\alpha_2-\frac{\Upsilon_1}{\Upsilon_2}\sin\alpha_1\sin\alpha_2, \tag{25}$$

$$\chi=\sin\alpha_1\cos\alpha_2+\frac{\Upsilon_1}{\Upsilon_2}\cos\alpha_1\sin\alpha_2, \tag{26}$$

$$\zeta=\sin\alpha_1\cos\alpha_2+\frac{\Upsilon_2}{\Upsilon_1}\cos\alpha_1\sin\alpha_2, \tag{27}$$

$$\mu=\cos\alpha_1\cos\alpha_2-\frac{\Upsilon_2}{\Upsilon_1}\sin\alpha_1\sin\alpha_2, \tag{28}$$

also $\Upsilon_j=\rho_j\beta_j^2k_j$, $\alpha_j=k_jd_j$, $j=1,2$, and d_j is the layer width. The subindex 1(2) labels the barrier (well)-acting material. N is the number of periods $d=d_1+d_2$. The phase of the transmitted amplitude $A_t=|A_t|e^{i\alpha_t}$ is equal to

$$\alpha_t=-k_2Nd+\arctan\left[\frac{h_+S(N)}{2C(N)}\right], \tag{29}$$

where

$$h_\pm=\frac{\Upsilon_2}{\Upsilon_1}\chi\pm\frac{\Upsilon_1}{\Upsilon_2}\zeta. \tag{30}$$

On the other hand, the coefficient of the solution at the X detector is equal to

$$A_r=\frac{[h_--i(\lambda-\mu)]S(N)}{h_+S(N)+2iC(N)}, \tag{31}$$

and the corresponding reflection phase is

$$\alpha_r=-k_2d_2+\arctan\left[\frac{h_+S(N)}{2C(N)}\right]-\frac{\pi}{2}. \tag{32}$$

Similar to Ref. 32, the transmitted and reflected time-dependent phonon packets are defined as

$$u_T(x,t)=\int\frac{dk}{2\pi}\phi(k)|A_t|e^{i[kx-\omega t+\alpha_t]}, \tag{33}$$

$$u_R(x,t)=\int\frac{dk}{2\pi}\phi(k)|A_r|e^{-i[kx+\omega t-\alpha_r]}, \tag{34}$$

where $\phi(k)$ is the phonon packet in the wave-vector space, defined as the Fourier transform of the phonon displacement describing the incident packet. It is assumed that the phonon packet is peaked around $k=k_0$. In the stationary phase approximation the peaks of the transmitted and reflected packets move according to

$$x=v_g\left(t-\left.\frac{d\alpha_t}{d\omega}\right|_{k_0}\right), \tag{35}$$

$$x=-v_g\left(t-\left.\frac{d\alpha_r}{d\omega}\right|_{k_0}\right), \tag{36}$$

where $v_g=d\omega/dk$ is the phonon group velocity. Scattering by the heterostructure causes temporal delays for the transmitted and reflected packets

$$t_{ph}^t=\left.\frac{d\alpha_t}{d\omega}\right|_{k_0}, \tag{37}$$

$$t_{ph}^r=\left.\frac{d\alpha_r}{d\omega}\right|_{k_0}, \tag{38}$$

which can be calculated from (29) and (32). In this way we generalize the results of Mizuno and Tamura for acoustic phonons to include optical phonons.[32]

For the sake of simplicity we are assuming that the origin of the superlattice is at $x=0$. The phases are sensitive to the location of the SL, i.e., they change as we shift the origin of the SL. This shifting also occurs for the electrons, see for example, Appendix A of Ref. 2 and Ref. 26, and will be useful in the next section.

Finally, let us recall the transmission and reflection coefficients reported in Ref. 33,

$$\mathcal{T}=-\rho_2\omega\beta_2^2k_2|A_t|^2/j_i=|A_t|^2=\frac{1}{C(N)^2+\dfrac{h_+^2}{4}S(N)^2}, \tag{39}$$

$$\mathcal{R}=-\rho_2\omega\beta_2^2k_2|A_r|^2/j_i=|A_r|^2=1-\mathcal{T}, \tag{40}$$

where $j_i=-\rho_2\omega\beta_2^2k_2$ is the incident flux.

IV. RELATION BETWEEN DWELL TIME AND PHASE TIMES

For an arbitrary configuration of barriers and wells between two semi-infinite media (the substrate and detector layers of well-acting materials) it is possible to find the following relationship between the dwell time and the phase times:

$$t_D\mathcal{T}=\tau_t\mathcal{T}+\tau_r\mathcal{R}+\tau_i, \tag{41}$$

where

$$\tau_t=-\frac{d\alpha_t}{d\omega}-\frac{b-a}{v_g}, \tag{42}$$

$$\tau_r = -\frac{d\alpha_r}{d\omega} + \frac{2a}{v_g}, \tag{43}$$

$$\tau_i = \frac{\omega_0^2}{\omega\beta^2 k^2}\sqrt{\mathcal{R}}\,\sin(\alpha_r - 2ka), \tag{44}$$

and the group velocity is $v_g = -\beta^2 k/\omega$. The proof is similar, from the mathematical point of view, to the calculations presented in Ref. 2, and is sketched in the Appendix. Note that (41) is identical to the one obtained for electrons (5) in Refs. 22 and 23, as previous1y discussed.

We call τ_t and τ_r total transmission and reflection times, respectively, or shortly transmission and reflection times. They are function of the time delays defined above (37), (38). Note that the total phase times refer to the extrapolated phase times of Ref. 2, i.e., they are the linear extrapolation to the local region of the heterostructure of the asymptotic phase times which are defined for a region with an extent large compared to the spatial extend of the wave packet. The relation (41) is still valid for a region (a,b) including not only the heterostructure but also a large region where there is not scattering potential, see the Appendix. In this extended region the phase times show their asymptotic character. We know the dwell time is a local quantity defined as function of the energy and the flux in each particular layer. In order to understand the meaning of τ_i, we can substract both the energy density of the incident phonon $\mathcal{H}_I$ and the energy density of the reflected wave $\mathcal{H}_R$ from the energy density at the heterostructure left side $\mathcal{H}_L$, and integrate this difference from the point $-L$, when L tends to infinity, to an arbitrary point x_1 to the left of the heterostructure. After dividing by the incident flux j_i we obtain

$$\begin{aligned}\Delta t_D &= -\frac{1}{j_i}\lim_{L\to\infty}\int_{-L}^{x_1}(\mathcal{H}_L - \mathcal{H}_I - \mathcal{H}_R)dx \\ &= -\frac{\omega_0^2}{\omega\beta^2 k^2}\sqrt{\mathcal{R}}\,\sin(\alpha_r - 2kx_1),\end{aligned} \tag{45}$$

showing that τ_i is an interference term (or time) coming from the overlap of the incident and reflected waves in from of the heterostructure. Knowing that, we can substract from the asymptotic phase times those parts corresponding to free motion, coming back to a region that only includes the heterostructure.

Given that our heterosystem is embedded in two semi-infinite media of well-acting materials we suppose, without any loss of generality, that the system has one barrier both at the beginning and at the end. It is straightforward to prove that both the transmission and reflection phases (α_t and α_r), computed for the periodic finite superlattice in the preceding section do not change if we remove the last well. Then we only need to consider that the length of the systems is now $b-a=Nd-d_2$, and we obtain that the total transmission time equals the total reflection time, $\tau_t = \tau_r$. Note that in the preceding section we suppose the heterosystem begins at $x=0$, thus we have here $a=0$. For a different from zero it is straightforward to prove that the phases shift conveniently and the relation $\tau_t=\tau_r$ is still fulfilled. Using the identity $\mathcal{T}+\mathcal{R}=1$ the above relation (41) simplifies to

$$t_D\mathcal{T} = \tau_t + \tau_i. \tag{46}$$

Following the method of Ref. 26 based on the time-reflection symmetry and the conservation of the density flux can be easily proven that also for phonons the total times are equal only for symmetric potentials. We mean by symmetric potential the case where the same material is used for both emitter and detector layers.

For the resonances, i.e., $\mathcal{T}=1$ and $\mathcal{R}=0$, the last term of (41) vanishes and $t_D=\tau_t$. The interference term is also zero for $\sin(\alpha_r)=0$. That implies

$$\frac{h_+}{2}\frac{S(N)}{C(N)} = -\cot(k_2 d_2) \tag{47}$$

and the transmission coefficient reads

$$\mathcal{T} = \frac{\sin^2(k_2 d_2)}{\cos^2(N\theta)}. \tag{48}$$

Note that τ_i is equal to zero for acoustic phonons. Thus the relation (46) is even simpler,

$$t_D = \frac{\tau_t}{\mathcal{T}}. \tag{49}$$

It is equivalent to the relation obtained for EM waves.[16] The replacements $\tau_t \to -\tau_t$ and $\tau_r \to -\tau_r$ in (42) and (43) are also needed for acoustical phonons when we follow the calculations of the Appendix for now $t_D = H/j$, as commented above.

Looking at the form of expression (49), the following is expected. First, t_D is proportional to the inverse of $\mathcal{T}$, and then the valleys (peaks) of t_D should correspond to the peaks (valleys) of $\mathcal{T}$. We will show later that the shape of τ_t resembles that of $\mathcal{T}$. That is also expected from the previous results for EM waves.[29] Then, at the peaks of $\mathcal{T}$, t_D should be a smoother function of the frequency when compared with τ_t. On the other hand, for the valleys of $\mathcal{T}$, the value of t_D at each frequency should be larger than the value of τ_t. It is known that as the number of barriers in the structure raises the valley in the transmission curve gets deeper.[33] Then, increasing the number of barriers the value of t_D should raise faster than the transmission time—for EM waves it is found in Ref. 29 that τ_t increases and tends asymptotically to a constant value. For the optical frequency range we find numerically that the contribution of the interference part is negligible at all frequencies, and the behavior discussed for acoustic modes should also be valid for the optical modes. These features are illustrated with numerical examples in the next section.

The type of relation here considered allows one to state an appropriate definition for the characteristic time involved in this problem and also when further complications appear, as for the oblique phonon incidence. This problem is now in progress.

V. DISCUSSION

To get insight into the physics of these systems it is worth to first consider both the one-barrier and double-barrier cases, for which analytical expressions for the dwell time and phase times can be easily obtained. These cases may help us to predict the behavior of larger systems. At the end of this section some numerical examples will be given

We start considering a phonon incident perpendicularly at one barrier of width ℓ. It is easy to check that at the frequency region where phonons in the barrier are allowed, the dwell time is equal to

$$t_D = \frac{1}{2\beta_1^2 k_1}[\omega\xi_+\ell + (\omega_{10}^2/\omega)\xi_- \sin(2k_1\ell)/2k_1], \qquad (50)$$

where $\xi_\pm = \rho\beta_1^2 k_1/(\rho_2\beta_2^2 k_2) \pm \rho_2\beta_2^2 k_2/(\rho\beta_1^2 k_1)$, and $k_1 = \sqrt{(\omega_{1\,0}^2 - \omega^2)/\beta_1^2}$ is the expression for the wave vector in the barrier. For frequencies forbidden in the barrier material it is only needed for the replacement $k_1 \to i\sqrt{(\omega^2 - \omega_{1\,0}^2)/\beta_1^2}$. It is also valid for the phase time. For acoustic phonons the dwell time is independent on the frequency, it grows linearly with the barrier width, and reads

$$t_D^{ac} = \xi_+^{ac}\ell/2v_1, \qquad (51)$$

where $\xi_\pm^{ac} = \rho_1 v_1/(\rho_2 v_2) \pm \rho_2 v_2/(\rho_1 v_1)$. We recall that we made the replacements $t_D \to -t_D$, $\omega_{1\,0} = \omega_{2\,0} = 0$, and $\beta_1^2 \to -v_1^2$, $\beta_2^2 \to -v_2^2$ to write it as a function of the sound velocities. Also here ρ_1 and ρ_2 refer to the total atomic masses.

For the phase times we have from (42), (43)

$$\tau_t = \tau_r = -\omega\left\{\frac{1}{4}\left(\frac{1}{\beta_2^2 k_2^2} - \frac{1}{\beta_1^2 k_1^2}\right)\xi_- \frac{\sin(2k_1\ell)}{1 + \frac{\xi_-^2}{4}\sin^2(k_1\ell)} - \left[\frac{\xi_+}{2\beta_1^2 k_1}\frac{1}{1 + \frac{\xi_-^2}{4}\sin^2(k_1\ell)}\right]\ell\right\}. \qquad (52)$$

For both acoustic and optical phonons the phase times show an oscillatory character, though the first term vanishes for acoustic phonons (given that $\beta_1 k_1 = \beta_2 k_2$). Also for nonpropagating optical states and ℓ tending to infinity, τ_t converges to a constant value (Hartman effect).

For the system composed by two barriers, with an inner well (both barrier and well of width ℓ) we obtain for the last barrier to the right (assuming left phonon incidence) an expression identical to (50), as expected. For t_D in the quantum well we have

$$t_D^{\text{well}} = \frac{1}{4\beta_2^2 k_2}\left\{\omega\ell[\xi_+^2 - \xi_-^2\cos(2k_1\ell)] + \frac{\omega_{2\,0}^2\xi_-}{\omega k_2} f(k_1,k_2)\right\}, \qquad (53)$$

where

$$f(k_1,k_2) = 2\sin(k_2\ell)^2\sin(2k_1\ell) + \xi_+\sin(k_1\ell)^2\sin(2k_2\ell). \qquad (54)$$

For acoustic phonons the second term in (53) vanishes, and we find the maxima of t_D at the resonances $2k_1\ell = (2n+1)\pi$, where n is an integer. The frequency values are at $\omega = v_1(n+1/2)\pi/\ell$. These resonances depend on the parameters of the barrier material and correspond to the minima in the transmission coefficient curves. Increasing the number of wells, the degenerate resonant states in each well hybridize to form new resonant states for the whole structure. A similar behavior is expected for the optical modes, as will be confirmed by numerical examples.

We study numerically the $(^{74}\text{Ge})_4$-$(^{70}\text{Ge})_4$ finite superlattices, previously considered in Refs. 31 and 33, for the reasons explained in the Introduction. The same input parameters as in Refs. 31 and 33 are used. In Figs. 1–3 the dwell time (solid lines) and the transmission times (dashed lines) as functions of the phonon frequency given in cm^{-1} are depicted for acoustic and optical phonons in the isotopic Ge finite superlattice. In Fig. 1 the acoustic phonons are shown, while in Figs. 2 and 3 the optical phonons for the allowed (Fig. 2) and forbidden (Fig. 3) frequency regions are presented. In order to clarify the meaning of both times we also plot the transmission coefficient $\mathcal{T}$ as a function of the phonon frequency. As noted in Ref. 33, $\mathcal{T}$ describes the behavior of the phonon modes. We increase in the calculations the number of barriers from 2 to 15. In Ref. 33 it was found that for 15 barriers the characteristics of the phonon modes are close enough to the dispersion relation of the infinite periodic system.

The most significant feature in Fig. 1 is the existence of a gap for the phonon modes (equivalent to a valley for $\mathcal{T}$), that is narrower and deeper for larger systems. The phase time shows the same behavior as $\mathcal{T}$. The dwell time presents characteristic peaks, indicating that the phonon spends more time in the heterosystem for these frequencies. With the exception of the modes in the gaps, the acoustic phonons have transmission coefficients very close to one. In Fig. 1(d) we represent $\mathcal{T}$ for 15 barriers with a dashed line in order to differentiate the peaks. In the inset of graphic Fig. 1(a) the peaks of τ_t for the 15 barriers system are shown. Note that t_D is the envelope of these peaks of τ_t. As commented before, this smoother behavior is expected from relation (49). Also t_D increases faster than τ_t when the size of the system is increased.

Figure 2 shows the case of optical phonon modes in the frequency range allowed to propagate in both the well and barrier layers. This is the same physical situation found for acoustic modes. The differences here come from the new dispersion relation of optical modes. The new feature in the dwell time is the divergences appearing when the frequency approach the value corresponding to the bulk material ($301.5\ \text{cm}^{-1}$). The transmission coefficient tends to zero when approaching this frequency value.

Figure 3 shows the case of optical phonon modes in the frequency range forbidden in the barrier layer and allowed in the well one. We pay attention here to the resonances result-

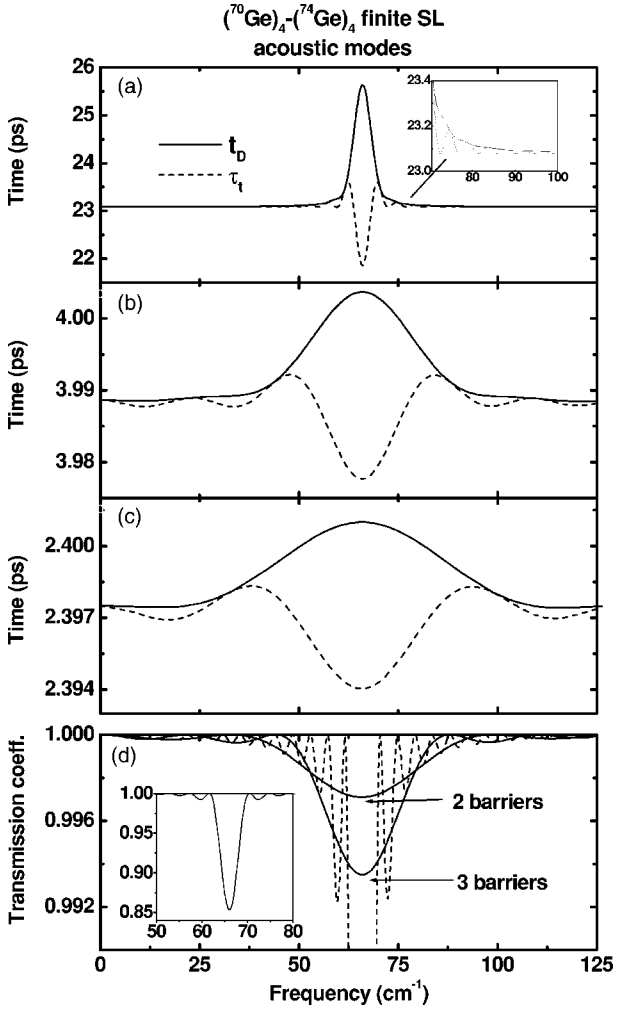

FIG. 1. The dwell time (solid line) and the transmission time (dashed line), both in ps, are plotted as a function of the acoustic phonon frequencies (in cm^{-1}) for the $(^{74}Ge)_4$-$(^{70}Ge)_4$ finite superlattice, with two (c), three (b), and 15 (a) barriers. In (d) the transmission coefficient is given for comparison. For the sake of clarity the transmission coefficient for 15 barriers is both plotted with dashed lines and shown in the inset. The upper inset shows some details of the times for 15 barriers.

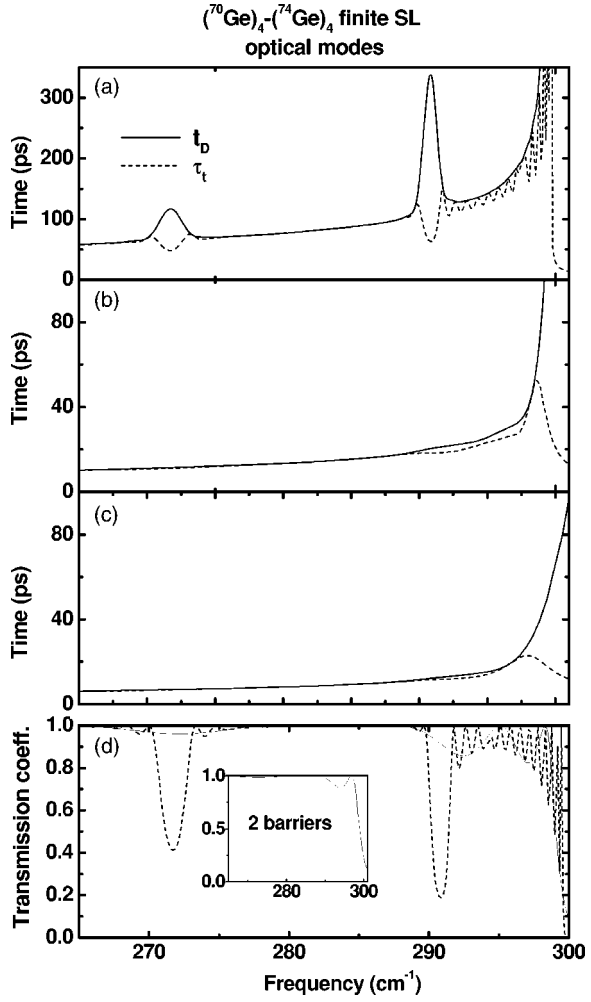

FIG. 2. The same as Fig. 1 for the allowed optical phonon states. For the sake of clarity the transmission coefficient for 15 barriers is plotted with dashed lines and for two barriers is shown in the inset.

ing from the presence of inner wells between the barriers. Given the hybridization of the modes, the resonance, that appears for the well in the double-barrier system at $\sim$305.57 cm^{-1}, is duplicate for the system with three barriers and two inner wells. The number of peaks increases for larger systems. Here it is clearly observed that the dwell time is the envelope function of the phase time. Also both times are equal at the resonances, as proved above. This behavior is found for all the figures. Here the order of magnitude of t_D and τ_t is 3 times larger than for both acoustic and allowed optical phonons. In general it is found that the time values for optical phonons are larger than for acoustic phonons. It is also worth noticing in Fig. 4 the small values of the interference term τ_i, which are much smaller than both t_D and τ_t for all optical modes.

VI. CONCLUSIONS

We have derived the dwell time that characterizes the tunneling for long wavelength phonons in semiconductor heterostructures from the energy density continuity equation. It is related to the vibrational energy stored in the heterostructure during the tunneling process. We also derived an analytical relationship between the dwell time t_D and the phase time τ_t. This result helps to clarify the meaning of both times. In general it is found that both times could be used to describe the features of the phonon modes. For optical phonons it is found that the magnitude of the time is larger than for acoustic phonons. Though for optical phonons the interference term—resulting from the overlap of incident and reflected waves in front of the heterostructure—is not zero (like for acoustic phonons), it has a small value. We also found that the dwell time is the envelope function of the peaks of the phase time for allowed states. In particular, t_D equals τ_t at the resonances. In Ref. 30 the Christoffel equations are employed to study a macroscopic system, i.e., the same equations used to study the long wavelength acoustic

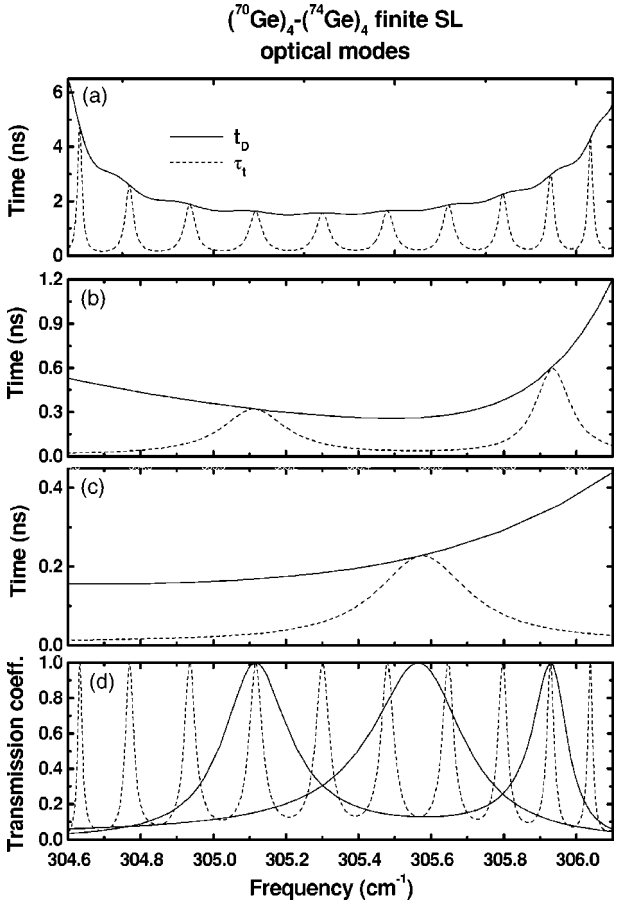

FIG. 3. The same as in the previous figures for the forbidden optical phonon states. The time is now in ns. For the sake of clarity the transmission coefficient for 15 barriers is plotted with dashed lines.

phonons. These authors also considered decoupled modes. They computed theoretically the transmission coefficients using the transfer matrix method and the group velocities simulating the propagation of waves packets. Their theoretical results are in agreement with their own experimental data. Given that we are also employing the speed of the sound in the media as input parameter, a qualitative check of the order of magnitude our times is obtained replacing the dimension of their system by the nanometric dimensions of our systems. The same order of magnitude of the times presented in Fig. 1 is obtained. Although more experimental evidence is needed. An experimental study of the features of the tunneling time from the allowed states to the gap of the bulk phonon modes could be useful. These oscillations are not easily detected in the experiment. Additionally, real structures have imperfections that destroy the interference pattern, and the small oscillations or peaks in the times, and also the interference term are not easily detected—in addition to the small oscillations for the allowed states and the different behavior of allowed and forbidden states. In this sense, the isotopic heterostructures (given their almost ideal interfaces) are the most valuable candidates for an experimental study. We hope that this work could motivate further experimental studies and possible applications.

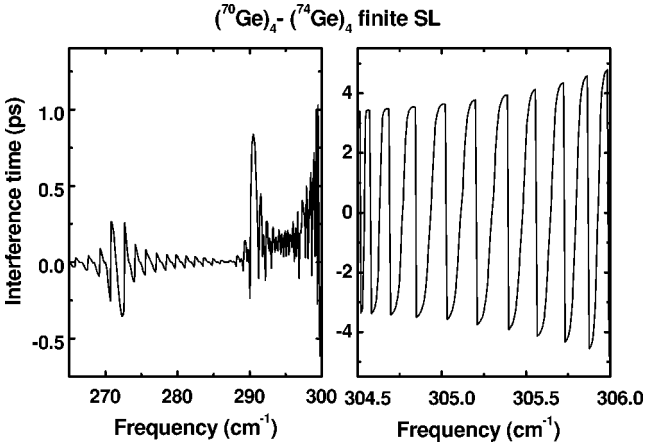

FIG. 4. The interference time (in ps) is plotted as a function of the phonon frequencies (in cm^{-1}) for the (^{74}Ge)$_4$-(^{70}Ge)$_4$ finite superlattice with 15 barriers.

On the other hand, given the mathematical analogy between the phonon problem and both the electronic tunneling and the propagation of EM waves, and despite the conceptual complications deriving an appropriate time for electrons, the findings reported in this paper could be easily extrapolated for these other systems.

ACKNOWLEDGMENT

The authors gratefully acknowledge H. Rodriguez-Coppola for useful and clarifying comments.

APPENDIX: DERIVATION OF THE RELATION BETWEEN THE DWELL TIME AND THE PHASE TIMES

Suppose we have an arbitrary configuration of barriers and wells in the spatial region (a,b), sandwiched between two semi-infinite well-acting materials. We employ the method developed in Refs. 2 and 24, taking advantage of the mathematical analogy between the stationary electron and phonon problems. The emphasis is here in the features characteristic of phonons. We integrate the continuity equation (9) across the region of interest for an arbitrary time-dependent energy density,

$$\frac{d}{dt}\int_a^b \mathcal{H}dx + j(b,t) - j(a,t) = 0. \tag{A1}$$

It is useful to cast the solution of the stationary equation of motion (8) in the form

$$u(x) = \begin{cases} e^{ikx} + A_r(k)e^{-ikx}, & x \leqslant a, \\ \Psi(x,k), & a < x < b, \\ A_t(k)e^{ikx}, & x \geqslant b, \end{cases} \tag{A2}$$

and to write the Fourier decomposition for each part of the solution with weights determined by the Fourier transform of the initial wave packet,

$$u_L(x,t) = \int \frac{dk}{2\pi}\phi(k)[e^{ikx} + A_r(k)e^{-ikx}]e^{-i\omega t}, \tag{A3}$$

$$u_{(a,b)}(x,t) = \int \frac{dk}{2\pi}\phi(k)\Psi(x,k)e^{-i\omega t}, \tag{A4}$$

$$u_R(x,t) = \int \frac{dk}{2\pi}\phi(k)A_t(k)e^{i(kx-\omega t)}, \tag{A5}$$

where the subscripts L (R) refer to the left (right) of the region (a,b). Substituting (A3)–(A5) in the expressions (6) and (10) to write (A1), assuming that initially the wave packet was at the left of $x=a$ and considering that the overlap with the interval (a,b) will be essentially zero, then (A1) can be integrated twice in time. In the time integration the relation

$$\delta(\omega-\omega') = \frac{1}{2\pi}\int_{-\infty}^{\infty} e^{-i(\omega-\omega')\tau}d\tau = \frac{(\omega+\omega')}{\beta^2(k+k')}\delta(k-k'), \tag{A6}$$

valid for the phonon dispersion relation $\omega^2=\omega_0^2-\beta^2k^2$, is employed. The first part of (A1) reads after the integration and for the stationary solution

$$\Pi_1 = \int dk \frac{|\phi(k)|^2}{2\pi}\left(\frac{\omega}{k\beta^2}\right)\int_a^b dx\mathcal{H}_{(a,b)}(k,x), \tag{A7}$$

where

$$\mathcal{H}_{(a,b)}(k,x) = \frac{1}{2}\rho\left|\frac{\partial\Psi}{\partial t}\right|^2 + \frac{1}{2}\rho\omega_0^2|\Psi|^2 - \frac{1}{2}\rho\left|\frac{\partial\Psi}{\partial x}\right|^2. \tag{A8}$$

Both the second and third part of (A1) involve larger terms. The integration in either k or k' is easier by changing to the variables $k=Q+q/2$ and $k'=Q-q/2$. The calculations are lengthly but straightforward and lead to

$$\Pi_2 = -\int \frac{dk}{2\pi}|\phi(k)|^2\rho\omega^2\left[|A_t(k)|^2\tau_t(k) + |A_r(k)|^2\tau_r(k) + \frac{\omega_0^2}{\omega\beta^2k^2}|A_r(k)|\sin(\beta(k)-2ka)\right], \tag{A9}$$

where $\tau_t(k)=-d\alpha_t(k)/d\omega-(b-a)/v_g$ and $\tau_r(k)=-d\alpha_r(k)/d\omega+2a/v_g$. From (A1) we have the condition $\Pi_1+\Pi_2=0$. Given that $|\phi(k)|^2$ is essentially arbitrary the relation (41) is obtained.

*Electronic address: villegas@uclv.edu.cu
†Electronic address: fernando@theo3.physik.uni-stuttgart.de
‡Electronic address: rpa@fisica.uh.cu

[1] C. A. A. de Carvalho and H. M. Nussenzveig, Phys. Rep. **364**, 83 (2002).
[2] E. H. Hauge and J. A. Støvneng, Rev. Mod. Phys. **61**, 917 (1989).
[3] V. S. Olkhovsky and E. Recami, Phys. Rep. **214**, 339 (1992).
[4] R. Y. Chiao and A. M. Steinberg, in *Progress in Optics*, edited by E. Wolf (Elsevier, Amsterdam, 1997), Vol. XXXVII, p. 345.
[5] R. Landauer, Nature (London) **341**, 567 (1989).
[6] Th. Martin and R. Landauer, Phys. Rev. A **45**, 2611 (1992).
[7] A. M. Steinberg, P. G. Kwiat, and R. Y. Chiao, Phys. Rev. Lett. **71**, 708 (1993).
[8] Ch. Spielmann, R. Szipöcs, A. Stingl, and F. Krausz, Phys. Rev. Lett. **73**, 2308 (1994).
[9] M. Mojahedi, E. Schamiloglu, F. Hegeler, and K. J. Malloy, Phys. Rev. E **62**, 5758 (2000).
[10] S. Longhi, M. Marano, P. Laporta, and M. Belmonte, Phys. Rev. E **64**, 055602(R) (2001).
[11] G. Nimtz, A. Enders, and H. Spieker, J. Phys. I **4**, 565 (1994).
[12] A. Enders and G. Nimtz, J. Phys. I **2**, 1693 (1992); **3**, 1089 (1993).
[13] A. Ranfagni, D. Mugnai, P. Fabeni, and G. P. Pazzi, Appl. Phys. Lett. **58**, 774 (1991).
[14] Ph. Balcou and L. Dutriaux, Phys. Rev. Lett. **78**, 851 (1997); J. J. Carey, J. Zawadzka, D. A. Jaroszynski, and K. Wynne, *ibid.* **84**, 1431 (2000).
[15] M. S. Bigelow, N. N. Lepeshkin, and R. W. Boyd, Science **301**, 200 (2003); L. J. Wang, A. Kuzmich, and A. Dogariu, Nature (London) **406**, 277 (2000); D. R. Solli, C. F. McCormick, C. Ropers, J. J. Morehead, R. Y. Chiao, and J. M. Hickmann, Phys. Rev. Lett. **91**, 143906 (2003); I. Alexeev, K. Y. Kim, and H. M. Milchberg, *ibid.* **88**, 073901 (2002); A. Kuzmich, A. Dogariu, L. J. Wang, P. W. Milonni, and R. Y. Chiao, *ibid.* **86**, 3925 (2001).
[16] H. G. Winful, Opt. Express **10**, 1491 (2002), http://www.opticsexpress.org/abstract.cfm?URI=OPEX-10-25-1491
[17] H. G. Winful, Phys. Rev. Lett. **90**, 023901 (2003).
[18] H. G. Winful, IEEE J. Sel. Top. Quantum Electron. **9**, 17 (2003).
[19] H. G. Winful, Phys. Rev. E **68**, 016615 (2003).
[20] T. E. Hartman, J. Appl. Phys. **33**, 3427 (1962).
[21] P. Krekora, Q. Su, and R. Grobe, Phys. Rev. A **64**, 022105 (2001).
[22] H. G. Winful, Phys. Rev. Lett. **91**, 260401 (2003).
[23] E. H. Hauge, J. P. Falck, and T. A. Fjeldly, Phys. Rev. B **36**, 4203 (1987).
[24] F. T. Smith, Phys. Rev. **118**, 349 (1960).
[25] M. Büttiker, Phys. Rev. B **27**, 6178 (1983).
[26] J. P. Falck and E. H. Hauge, Phys. Rev. B **38**, 3287 (1988).
[27] M. A. Moura and M. de Albuquerque, Solid State Commun. **74**, 353 (1990).
[28] S. Esposito, Phys. Rev. E **64**, 026609 (2001).
[29] P. Pereyra, Phys. Rev. Lett. **84**, 1772 (2000).
[30] W. M. Robertson, C. Baker, and C. B. Bennett, Am. J. Phys. **72**, 255 (2004); W. M. Robertson, J. Ash, and J. M. McGaugh, *ibid.* **70**, 689 (2002); J. N. Munday, C. B. Bennett and W. M. Robertson, J. Acoust. Soc. Am. **112**, 1353 (2002).
[31] F. de León-Pérez and R. Pérez-Alvarez, Phys. Rev. B **61**, 4820 (2000).
[32] S. Mizuno and S. I. Tamura, Phys. Rev. B **50**, 7708 (1994).
[33] F. de León-Pérez and R. Pérez-Alvarez, Phys. Rev. B **63**, 245304 (2001).
[34] S. Tamura and S. Mizuno, Physica B **263–264**, 455 (1999).

[35] K. Imamura, Y. Tanaka, and S. Tamura, Physica B **316–317**, 234 (2002).

[36] V. Narayanamurti, Science **213**, 717 (1981).

[37] J. Spitzer, T. Ruf, M. Cardona, W. Dondl, R. Schorer, G. Abstreiter, and E. E. Haller, Phys. Rev. Lett. **72**, 1565 (1994); J. Spitzer, Ph.D. thesis, University of Stuttgart, 1994. For a review see E. E. Haller, J. Appl. Phys. **77**, 2857 (1995).

[38] For a study of the zinc-blend structure see, for example, A. Fasolino, E. Molinari, and K. Kunc, Phys. Rev. B **41**, 8302 (1990). The diamond structure is a particular case of the former with two equal atoms in the elemental cell.

[39] Most spectroscopic techniques are able to measure long-wavelength phonons, see for example, B. Jusserand and M. Cardona, in *Light Scattering in Solids V*, edited by M. Cardona and G. Güntherodt (Springer-Verlag, Heidelberg, 1989).

[40] C. Trallero-Giner, R. Pérez-Alvarez, and F. García-Moliner, *Long Wave Polar Modes in Semiconductor Heterostructures* (Pergamon/Elsevier Science, London, 1998).